





# Automatic Large-Scale Precise Mapping and Monitoring of Agricultural Fields at Country Level With Sentinel-2 SITS

Yady Tatiana Solano-Correa , *Member, IEEE*, Khatereh Meshkini , *Student Member, IEEE*,  
Francesca Bovolo , *Senior Member, IEEE*, and Lorenzo Bruzzone , *Fellow, IEEE*

**Abstract**—Availability of multitemporal (MT) images, such as the sentinel-2 (S2) ones, offers accurate spatial, spectral and temporal information to effectively monitor vegetation, more specifically agriculture. Agricultural practices can benefit from temporally dense satellite image time series (SITS) for accurate understanding of the phenological evolution and behavior of crops. Developing techniques that deal with high spatial correlation and high temporal resolution requires a shift in the processing paradigm and poses new challenges in terms of data processing and methodology. This article presents an automatic approach to large-scale precise mapping of small agricultural fields based on the analysis of S2-SITS at Country level. The approach deals with a flexible and automatic processing chain for massive data and was tested at Country level. The large-scale application requires to consider: the management of big amount of data with particular attention to download and pre-processing of S2-SITS; and MT fine characterization of crop fields accounting for the strong variability in size and phenological behaviors when mapping at large scale. Both challenges are addressed in an automatic way by exploiting and/or updating state-of-the-art methodologies. Promising results have been obtained and validated over 2017 and 2018 agrarian years for Italy.

**Index Terms**—Large-scale mapping, multitemporal (MT), precision agriculture, satellite image time series (SITS), sentinel-2 (S2).

## I. INTRODUCTION

**N**OWADAYS the access to multitemporal (MT) remote sensing (RS) images at high spatial and spectral resolution has greatly improved (e.g., with S2 data), resulting in a high amount of information for large-scale mapping with high accuracy. In addition to advances in the technology for

Manuscript received October 25, 2021; revised January 27, 2022 and March 25, 2022; accepted March 29, 2022. Date of publication April 4, 2022; date of current version May 3, 2022. This work was supported by ESA under the Project Scientific Exploitation of Operational Missions (SEOM) - S2-4SCI - Land and Water-Multi-Temporal Analysis. (*Corresponding author: Francesca Bovolo.*)

Yady Tatiana Solano-Correa and Francesca Bovolo are with the Fondazione Bruno Kessler, Center for Information and Communication Technology, 38123 Trento, Italy (e-mail: tsolano@unicauca.edu.co; bovolo@fbk.eu).

Khatereh Meshkini is with the Fondazione Bruno Kessler, Center for Information and Communication Technology, 38123 Trento, Italy, and also with the Department of Information Engineering and Computer Science Trento, University of Trento, 38123 Trento, Italy (e-mail: mkhatereh@fbk.eu).

Lorenzo Bruzzone is with the Department of Information Engineering and Computer Science Trento, University of Trento, 38123 Trento, Italy (e-mail: lorenzo.bruzzone@ing.unitn.it).

Digital Object Identifier 10.1109/JSTARS.2022.3164547

RS data collection, there have been important scientific and methodological developments in processing the vast quantity of MT RS data [1]. In this article, two issues exist: data preparation and data exploitation. The former guarantees homogeneity and reliability of data from download to pre-processing, and includes data quality check. As the spatial scale of analysis becomes larger (i.e., Country or continental level), this step should become completely automatic and flexible [2]–[5]. The latter deals with the generation of user dependent informative layers. Most activities in this article have been based on supervised machine learning that rely on training samples [6]–[9]. Training samples collection is a critical problem which scales up as scale becomes larger (e.g., multiple S2 tiles or Country level) [10] and time series longer. Furthermore, supervised machine learning methods work effectively when applied on a user-defined study area, but they tend to fail (despite transfer learning and domain adaptation paradigms) when applied across large space and time scales [11]–[14]. This happens because the target classes are highly variable and embedded in a heterogeneous and complex natural or anthropogenic landscape, and insufficient training samples are available to adequately represent the high and fast spatio-temporal variability. Agricultural areas are an example of significant variability across space and time, even over small scales (for example inside the same Country) in terms of both size and phenological behaviors over time.

In the era of big data, data preparation and homogeneity requires methods and platforms for a better and easier management [2], [5], [15]. In the case of United States, in March 2012, the government proposed the “Big Data” initiative. This project focuses on improving the ability to extract knowledge from large and complex collections of digital data [16]. In the specific case of RS, the Earth Observing System Data and Information System [17] project is the one to provide end-to-end solutions for managing NASA’s Earth science data. This program is one of the most advanced ones at the moment, but does not offer a high performance computing (HPC) option, letting the task of processing to the users. For Europe, in 2013, the European Commission adopted the largest research and innovation program “Horizon2020” to support the implementation of big data related projects. In this article, several projects have been launched in order to guarantee availability and management of platforms for HPC and data storage [2], [5], [15], [18], [19]. Several other institutions and agencies have been investing in the same direction. Such is the case of the European Space Agency (ESA)

that through the Copernicus program makes use of the data and automation access services (DIAS) platforms/environments [2], in order to process all their Earth Observation data. DIAS allows to access/process most of the Copernicus Sentinel satellites data and services, but also has some limitations due to costs, full availability of processed/corrected data and or corrupted data systems. An alternative to NASA and ESA is the Google Earth Engine platform [15], that is a planetary-scale platform for Earth science data and analysis. It makes available most of the open access satellite data from the global space agencies and allows online analysis/processing/access of/to data. It has some limitations (given its free nature) in terms of amount of data that can be processed and downloaded and in terms of highest processing level data availability. Such is the case of S2 L2A level, only available since March 2017, thus limiting analysis of older data [20]. Therefore, local strategies are required that allow us to handle and process the data in an automatic and effective way. Every existing service has possible limits, but any can be used depending on user needs and possibilities.

Preprocessed and homogenized data become the input for information extraction. In the specific case of precision agriculture, several efforts have been made in the literature to map information at both small and large spatial scales. This includes both identification and separation of single crop fields and extraction of phenological information for agricultural areas mapping. A crop mapping method effective on different agricultural areas in China was proposed in [21]. The algorithm applies an adaptive Savitzky–Golay filter to smooth enhanced vegetation index time series derived from MODIS surface reflectance data and an iterative time moving-window to map the crop cycles. Another study proposed a hierarchical crop mapping protocol, which applies a decision tree to MODIS normalized difference vegetation index (NDVI) time series for large-area crop mapping in US [9]. However, the spatial resolution of MODIS is too coarse for small crop fields. Other researchers have focused on satellites with higher spatial resolution (30 m or higher) to produce detailed cropland maps for both large and small crop fields [22]–[29]. Yan and Roy [22], [28], proposed a web enabled landsat data time series object-based approach to enable a robust agricultural field segmentation together with a watershed algorithm to decompose connected segments belonging to multiple fields in Texas, California and South Dakota. While this method works at high spatial resolution, it has been applied to large single cropping cycle fields (US scale) only. In [23], a detailed spatial analysis is presented that is able to extract subboundaries over already detected crop fields. To do so, the method heavily relies on an already existing crop field map and on high spatial resolution data from SPOT sensor (less than 5 m). Due to SPOT data availability, it is highly limited to small scale analysis. The Sen2Agri tool exists that is able to deal with both Landsat and S2 data and works at large-scale [29]. Sen2Agri generates annual cropland and crop type masks, but its accuracy is highly dependent on in-situ data and requires to download data locally. A first attempt to generate an automatic method that maps small crop fields (with S2 data) in an intensively cultivated area of Barrax in Spain has been proposed in [24], with further details presented on [25]–[27]. While the method removes some of the limitations from other existing methods in literature, it has been demonstrated on small-scale test site

only and under the assumption of no cloudy time series (cloudy images have been removed manually). Accordingly, there is the need to develop an end-to-end automatic strategy that allows to study large-scale areas with strong variability of crop-field size (from very large to very small ones) in an automatic way and adjustable to local/different conditions (e.g., phenology) arising from working at Country level.

This article aims at proposing a flexible and automatic crop mapping method by taking into account large-scale mapping challenges in S2 satellite image time series (SITS—high spatial resolution) at Country level [25], [30]. To achieve this goal, two research questions are targeted: how to handle big amount of data with particular attention to download and pre-processing of S2-SITS; and how to perform multitemporal fine characterization of crop fields accounting for the strong variability in size and phenological behaviors when mapping at large scale. The proposed approach deals with data preparation and preprocessing at large-scale from end-to-end by introducing a set of steps that guarantee reliable data. Moreover, the approach focuses the attention on precision agriculture of small crop fields (while preserving the capability of state-of-the-art methods to deal with large ones) and introduces robust strategies to handle high amount of large-scale data. The system has been applied to entire Italy for the 2017 and 2018 agrarian years (from November 2016 to October 2018) with S2-SITS in order to generate products for precision agriculture at Country level.

The rest of this article is organized as follows. Section II introduces the proposed method for precise mapping of small agricultural fields in large-scale with S2-SITS. Section III describes the dataset as well as the validation process. Section IV presents the general results for the entire Italy, as well as detailed results for the different stages on three S2 tiles over Italy, used for validation. Finally, Section V draws the conclusions and illustrates future works.

## II. PROPOSED APPROACH TO AUTOMATIC LARGE-SCALE MAPPING AND MONITORING OF AGRICULTURAL FIELDS WITH S2-SITS

The proposed approach addresses two main problems, being data preparation and data analysis. The former deals with the automatic download and pre-processing of S2 SITS, at large-scale, to guarantee reliable data. The latter deals with the characterization of agricultural areas with S2 images at both single/small and large crop field level accounting for strong phenological variability. The whole process applies at Country level in an automatic way, tile by tile, to parallelize (if processing infrastructure allows) and thus speed up the process. The only input from the user is a shape file of the Country and the agrarian year to be studied. Fig. 1 shows the block scheme of the proposed approach to precise mapping of small agricultural fields in large-scale S2 SITS. Details of each step are provided in the following section.

### A. S2-SITS Download and Pre-Processing at Large-Scale

The first step deals with data retrieval and reliability at Country level. The task is complex and requires a high automation level. Fig. 2 shows the block scheme of the proposed automatic

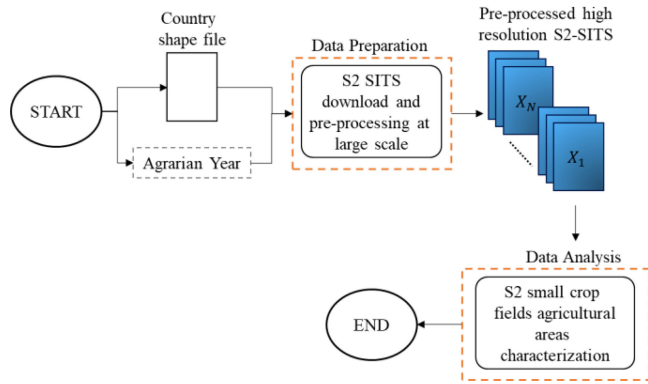


Fig. 1. General block scheme of the proposed method.

downloading and preprocessing of the S2 SITS at large-scale. The process has been designed to mitigate the impact of problems raising while working with large-scale data. Here, we take advantage of the official API documentation prepared by ESA in order to search, download and retrieve Sentinel satellite images from the copernicus open access hub (Sci-Hub). This option exists for any programming language (e.g., Python) [31], [32]. Taking into account the Country shape file and the agrarian year of interest, a list of tiles falling inside the area of interest is created and a parallel search is conducted tile by tile. The Sci-Hub limitation to download two images at the same time per user account (to ensure download capacity for all users [32]) creates a bottleneck on the processing chain. This is an issue that applies to any user working outside any project or without access to a DIAS, where data is usually already available.

Since information extraction over agricultural areas implies the use of physical variables, L2A images are required. With the list of tiles to download, the query starts by searching for available L2A level images. Since the amount of data acquired by the Sentinel sensors is huge, ESA has decided to start archiving some of the images acquired in the past. These images are still available under user request, and it takes around 24 h to obtain the access. Thus, the proposed algorithm places the request for data to download when it becomes available. As per ESA communication, S2 images at L2A level are not available for all the years/acquisitions, neither they will be in the near future. Therefore, once the querying and download process ends over available L2A images for each tile, it repeats the process for the L1C level images. Similar to L2A level images, there are some L1C images that have been archived, the same process as per L2A images is followed. While L2A images are already atmospherically corrected, L1C ones are not. The processing of L1C to L2A level can be performed by several methods, offering different quality levels [33]–[35]. The selection of processing method is up to the user. In this article, it is performed by automatically triggering the Sen2Cor v.2.5.5 (or higher) with SRTM DEM [35] routine.

Since the huge amount of data makes the probability of data corruption non-negligible, a step of data integrity verification is automatically conducted (i.e., no missing bands at any spatial resolution—see [36]—or no unadvertised corrupted images from Sen2Cor). The final step checks if all requested images from the archive have been downloaded and preprocessed. The

block scheme in Fig. 2 illustrates the procedure that mitigates the impact of the different problematics raised by working at large-scale. A maximum execution time and a new query of the processes is set to guarantee that the automatic procedure does not exceed temporal limits (e.g., running out of processing time, missing images at the time of query, etc.).

This step produces temporally dense SITS of S2 images acquired over the same geographical area in one agrarian year  $[t_1, t_N]$  with  $(n \in [1, N])$ . Let us define this output as  $SITS = \{X_1, X_2, X_3, \dots, X_N\}$ . Let us assume that  $X_n$  ( $n = 1, \dots, N$ ) in SITS has size  $I \times J$ . S2 SITS can be used for information extraction. Here we focus on a precise mapping of small crop fields in agricultural areas.

### B. Small Crop Fields Agricultural Areas Characterization

This step uses as input the pre-processed S2 SITS and an agricultural areas map. The latter can be of any origin and might sometime contain both agricultural areas and other vegetation classes with a similar behavior to that of crops. For example, it can be a cadastral map, an ad-hoc map generated for the considered test site (by photo-interpretation), a map derived from RS data, etc. These maps are usually built by considering single date information, thus being inaccurate or incomplete. Because of this, such maps are only used as an initial reference to be tuned by following steps. Inspired by the method in [24], here we introduce a set of implementations to work at large-scale (see Fig. 3). The small crop fields agricultural areas characterization at large-scale with S2 images is based on three main steps: spatio-temporal fusion; time series reconstruction, and crop parameter estimation. Let us assume that an agricultural area map is available; the area is intensively cultivated; different crop types are cultivated; and crop fields exits being small but have an area larger than 3-4 ha (because of S2 spatial resolution).

1) *Spatio-Temporal Fusion Step*: In this step, an MT crop field map is generated that contains only areas cultivated over an agrarian year. Given the S2-SITS a fusion is performed over space and time to detect spatio-temporal homogenous areas. In [24], spectral and spatial information derived from the NDVI is exploited in a cumulative way over the entire S2-SITS over a small area. While aggregating this information in time, the method applies two thresholds (one over the spectral variable and another over the spatial one) that allow to separate among crop fields by exploiting the temporal phenological behavior of vegetation. When applying the algorithms to several tiles (even neighboring ones), the method tends to fail both in terms of spatial and temporal locality, due to the variability of cultivation practices and the presence of crop fields with highly variable sizes (large to small). This problem becomes even more critical as the number of suitable S2 images varies abruptly from one agrarian year to another and as the scale becomes larger. To improve reliability and flexibility of the method over large-scale areas and with variable number of images, we designed a spatio-temporal fusion step as shown in Fig. 4. We use the agricultural area map for a first separation between regions dedicated to agriculture and those that are not. Since this map might contain other classes than just crops, it is tuned by analyzing the NDVI over time. Every NDVI image ( $X_{NDVI_n}$  ( $n \in [1, N]$ )) in a given SITS is evaluated according to a threshold  $0 < T < 1$  that

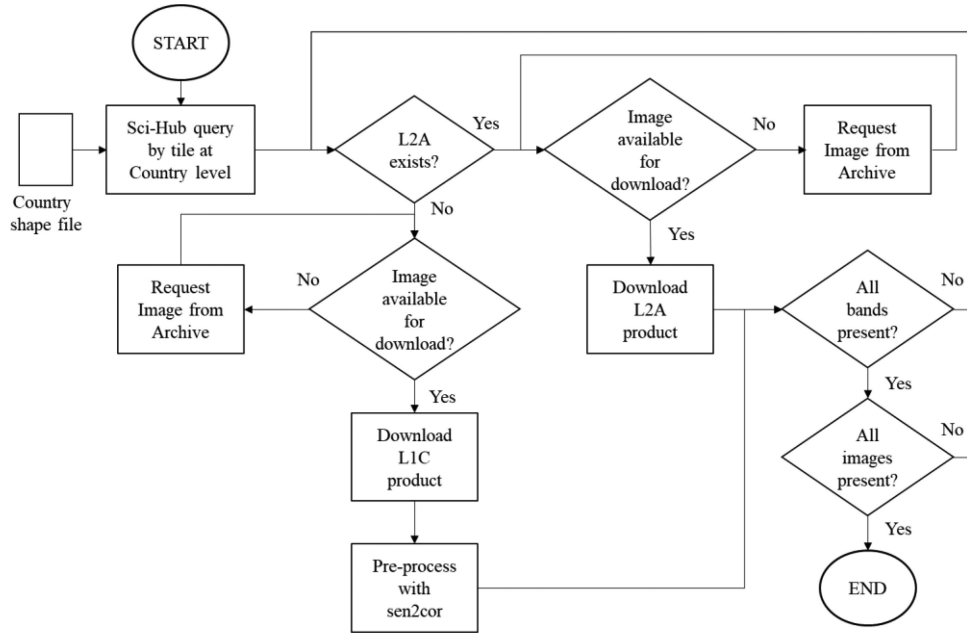


Fig. 2. Block scheme of the proposed S2 SITS download and preprocessing at large-scale.

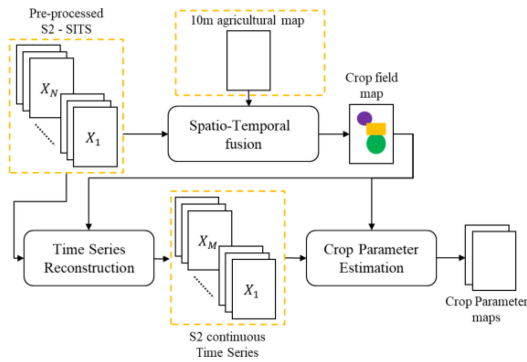


Fig. 3. Block scheme of the S2 agricultural areas characterization [24].

separates crops ( $\omega_c$ ) from other types of vegetation ( $\omega_{ov}$  – i.e., forest, grasslands and/or shrubs). The value of  $T$  is expected to remain the same along different agricultural areas. Therefore, it is rather easy to set it up by fast trial and error [24]. An MT cropland mask ( $X_{\text{cropland\_mask}}$ ) is therefore defined as

$$X_{\text{cropland\_mask}} = \begin{cases} \omega_c, & \text{if } \left( \sum_{n=1}^{n=N} (X_{\text{NDVI}_n} > T) \right) \geq 1 \\ \omega_{ov}, & \text{otherwise} \end{cases} \quad (1)$$

$X_{\text{cropland\_mask}}$  includes only cultivated areas in the studied agrarian year [24].

Let  $\Omega_f$  ( $f \in [1, F]$ ) be the set of  $F$  fields in SITS.  $\Omega_f$  includes both cultivated and fallow crop fields. Let us assume that crop fields in  $X_n$  ( $n \in [1, N]$ ) are cultivated with different types of crops, that intensive crop rotation is practiced in the area and that crop fields might be small, but not smaller than 3-4 ha (limit by S2 spatial resolution). Once the NDVI and the MT cropland mask (see Fig. 4) are extracted, the proposed approach proceeds as follows.

- 1) Extract the ten least-clouded images in the pre-processed S2 SITS equally distributed along the agrarian year. This selection is made based on the cloud coverage information offered by the scene classification map produced by Sen2Cor during the atmospheric correction process [35]. This step is performed only for the spatio-temporal fusion step and results in an equal number of images per year. This guarantees the processing of the same amount of data across different tiles in Italy.
- 2) Compute a gradient product collection by means of a Sobel operator in order to highlight crop boundaries. Other operators such as Prewitt, Roberts, Canny, Laplacian of Gaussian, Scharr and Hough can be used [24]. In our tests, the Sobel one was the one offering the best performance.
- 3) Compute the following.
  - a) Mean pixel gradient intensity.
  - b) Maximum pixel gradient intensity.
 This step is applied to reduce the variability across tiles in Italy.
- 4) Compute an edge intensity product ( $E(i, j)$ ) by multiplying the products obtained in steps 3.a and b;
- 5) Create a binary object-mask by thresholding  $E(i, j)$  ( $T_{\text{edge}}$ ) as

$$T_{\text{edge}} = k \times \frac{\sum_{i,j}^{I,J} E(i, j)_n}{I \times J} \quad (2)$$

where  $k$  is a factor that changes in an iterative way and  $E(i, j)$  is the edge intensity image.

- 6) Label the objects in the initial object-mask ( $X_{\text{mask}_1}$ ).
- 7) Compute the variance ( $\sigma^2$ ) of each object over the ten S2 images obtained in step 1.



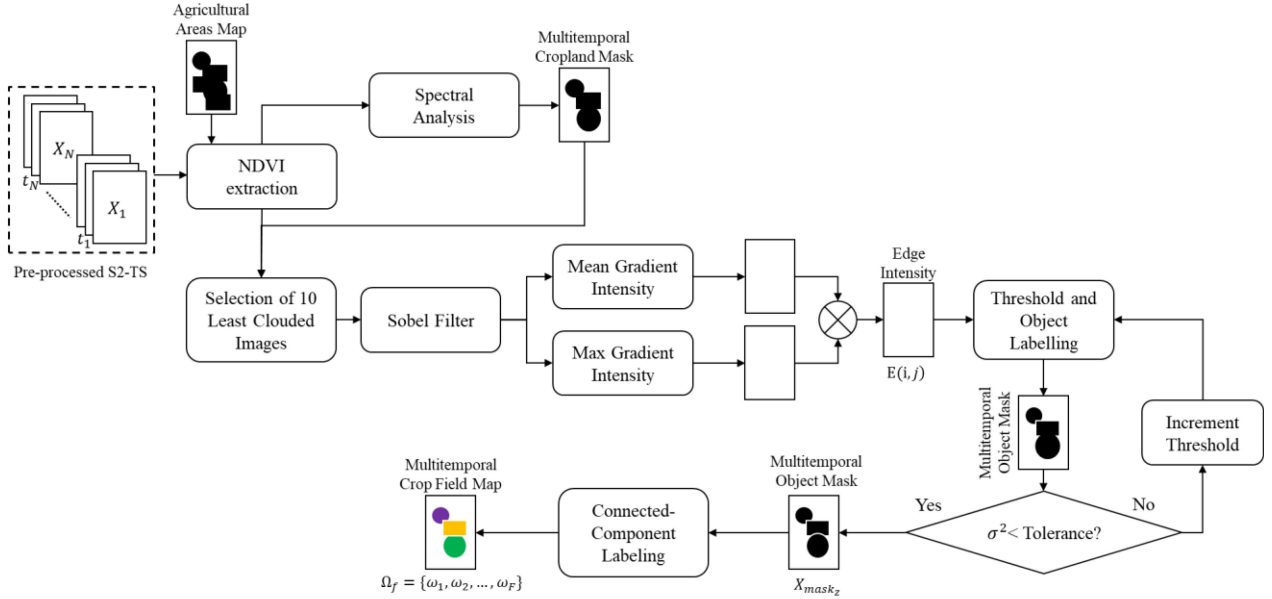


Fig. 4. Detailed block scheme for the spatio-temporal fusion step.

- 8) If  $\sigma^2$  of a given object is higher than a pre-set tolerance value ( $T_v$ ), then increment  $T_{edge}$  value. This is done by decreasing the value of  $k \in [2.0, 1.0, 0.75, 0.50, 0.25]$ .
- 9) Repeat steps 4 to 8 for all objects with  $\sigma^2 > T_v$ ;
- 10) Combine objects in an object mask  $X_{mask_z}$ , with  $z = k$  ( $k = 5$  in the steps).
- 11) Label the objects in  $X_{mask_z}$  to obtain the MT crop field map with  $\Omega_f = \{\omega_1, \omega_2, \dots, \omega_F\}$ .

Morphological steps are applied to each combination or thresholding stage in order to remove crop fields below a minimum area criterion. The proposed spatio-temporal fusion step allows for both a more robust generation of crop field map (w.r.t. what proposed in [24]) and a reduced computational time at tile level (ten times faster). The selection of parameters heavily impacts on error reduction. Different tests and trials were carried out in order to set up the steps.

2) *Time Series Reconstruction Step*: In this step, S2 SITS continuous in time are generated. This is done over the entire pre-processed S2 SITS (not over the ten least clouded images as in the spatio-temporal fusion step). Three steps are followed [24].

- 1) Definition and extraction of NDVI-SITS sets.
- 2) NDVI-SITS data imputation by upper-envelope and withdrawn strategy and.
- 3) Adaptive nonparametric regression of augmented NDVI-SITS based on a multilayer perceptron neural network.

Working over large-scale data means having higher data variability. Thus we observe seasonal (winter/summer) crops, crops with one or more cropping cycles, fallow crops, permanent crops (e.g., vineyards) and specific agricultural practices (e.g., hail nets on top of the crops) that affect the NDVI response. Not to mention the higher variability in atmospheric conditions that result in lack of information (i.e., due to too many clouds in a certain area). To mitigate these issues, and to render the method robust at large-scale and at different agrarian years, two strategies were followed:

- 1) Filtering out local NDVI minima from the upper-envelope NDVI-SITS (see [24] for details on how to obtain the upper-envelope curve). The filtering process consists on locating and eliminating from the NDVI-SITS spectral-index value smaller than a threshold (w.r.t. the immediate neighbors). If the NDVI value does not follow an ascending or descending trend from one date to another, then the spectral-index value is not informative w.r.t. the regression mechanism and the phenological cycle of crops. Thus, it can be removed without loss of information;
- 2) Using an effective non-parametric regressor like the general regression neural network (GRNN—[37]) with an adaptive regression strategy. The adaptive strategy consists in iterating over the Gaussian kernel standard deviation ( $\sigma$ ) in GRNN until the mean square error (MSE) (w.r.t. a linear regression) falls below a threshold value. The initial  $\sigma$  is chosen to be restrictive in a range  $[0,1]$ , thus favoring a greater NDVI-SITS smoothing factor. While the MSE value is greater than a given threshold,  $\sigma$  is decreased and the regression iterated. The initial  $\sigma$  can be also bigger than 1, thus taking more time to converge to the desired MSE. While testing the different  $\sigma$  values, it was found that a smaller  $\sigma$  allowed the GRNN to better mimic the linearly regressed NDVI-SITS, thus preserving more of the high frequency components of the original signal.

These two strategies make the approach more robust while moving from small to large scale. As for the spatio-temporal fusion step, the computational time was reduced (w.r.t. [24]) by implementing this strategy, together with the use of the *groupby(.)* function offered in the Pandas library for python [38], that demonstrated to be more efficient than others in combining, splitting, and conducting operations with time series and large amount of data. Such is the case of the time series reconstruction step, where mean NDVI values are calculated for every crop field. Any other function or strategy can be used instead with negligible impacts on the performance, but computational time.

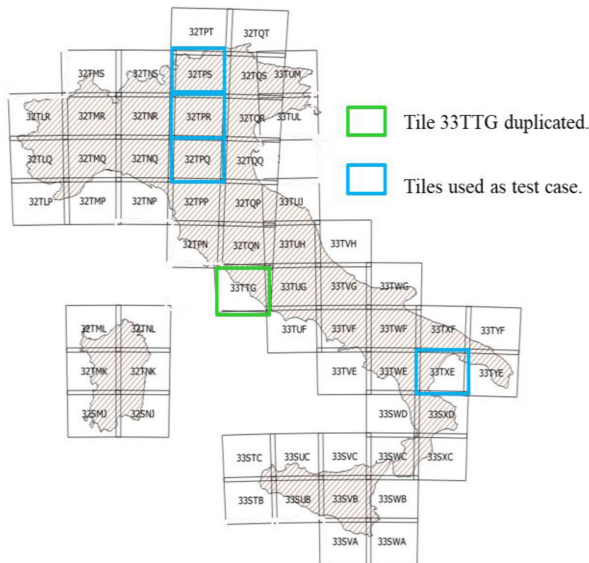


Fig. 5. Study area and corresponding S2 tiles.

3) *Crop Parameter Estimation Step*: In this step, phenological parameters are extracted at single crop field level, and thematic/informative maps are generated that allow for the detailed mapping and monitoring of agricultural areas. This is done by using the methodology in [27], given that the method is based on basic mathematical rules and the way in which the continuous NDVI-SITS are obtained does not affect them. Let us recall that the more precise the temporal series is (the closer the NDVI-SITS is to real acquisitions), the more precise the phenological parameters will be. Here, resides the relevance of implementing this step.

### III. STUDY AREA AND VALIDATION PROCESS

#### A. Dataset Description, Pre-Processing, and Ground Truth

The proposed approach was applied to S2-SITS acquired over Italy in the agrarian years 2017 (from November 2016 to October 2017) and 2018 (from November 2017 to October 2018) (see Fig. 5). The Italy-study area comprises 60 tiles or granules defined in the military grid reference system covering the entire Italian peninsula. Fig. 5 shows Italy (dashed silhouette) and the location of tiles required to cover the Italian territory with S2 images. S2 tiles are identified in the UTM projection and WGS 84 geographic coordinate system. Granule 33TTG (located over Rome) was removed due to the strong overlapping with the granule 32TQM (shown in light green square in Fig. 5). In practice, images from these two granules are duplicated. Taking into account the 60 tiles and the two agrarian years, a total of 19.660 images (data amount of about 12.97 TB—binary based unit, i.e., 1 TB = 1024 GB) were downloaded and processed. The time required to download and preprocess the data is highly dependent on internet connection and machine capacities. In our case, using a 16-cores processor with 16GB of RAM, we were able to perform this task in approximately 15 days.

TABLE I  
AVAILABLE S2 IMAGES PER TILE AND AGRARIAN YEAR

Tile	2017	2018
32TPS	108	202
32TPR	109	151
32TPQ	110	130
33TXE	82	79

#### B. Validation Datasets

A total of 4 out of the 60 available tiles (32TPQ, 32TPR, 32TPS, and 33TXE, as shown in Fig. 5) were used for validating the proposed approach. Their selection was based on maximizing agricultural areas variability (in terms of both crop-type to crop field area) over Italy and according to availability of open free reference information to validate. To give an idea of the variability among tiles and among years, Table I gives the total number of S2 images available per agrarian year and per tile (including cloudy images). Other than variation in number of tiles, we observe heterogeneity in terms of: number of crop fields; size of crop fields; environmental conditions (from alps to Padana Valley); and kind of cultivation. We further observe large fields in flat areas, medium to large fields in humid areas and small to medium fields in mountainous areas. Further details regarding the four tiles reference data are provided below.

1) *Emilia–Romagna Region—32TPQ Tile*: The validation dataset for the Emilia-Romagna region is published since 2008 by ARPAE and the Assessorato Agricoltura della Regione Emilia–Romagna [39]. They co-founded the Classificazione delle cOLture in atto tramite Telerilevamento project as a tool to identify and spatially quantify crops and the related water needs for the Emilia–Romagna region. The study area covers 11.800 km<sup>2</sup> and is focused on the agricultural area. The classification of crop fields is performed by means of the analysis of MT images acquired by optical satellite sensors (e.g., mainly U.K.-DMC2 and Deimos-1, Sentinel-2 and landsat 8 for areas occluded by clouds) from November to June of the considered agrarian year. A total of 14 crop-type classes are considered, and spatial details are limited to parcels owned by a farmer and not necessarily to the actual use of the field.

2) *Veneto Region—32TPR Tile*: The land-use data for the Veneto Region are collected and maintained by (Agenzia VEneta per i Pagamenti in Agricoltura, Venetian Agricultural Payments Agency—[40]). Here, we used the database dated October 21, 2020 available in [40]. The maps are generated by photointerpretation of RGB orthophotos acquired by AGEA in 2018 at a resolution of 20 cm or by means of *in situ* measurements performed using GPS instruments. In terms of land-use information, the land use legend is less detailed than CLC standard, but in terms of crop classification information, it is more detailed. It contains 171 unique classes mainly focused on the description of the agricultural area. Yet, the spatial detail w.r.t. single parcel/crop fields is not that high.

3) *Trentino Alto Adige Region—32TPS Tile*: The Trentino Region published in 2017 a high spatial resolution vector cartography map representing the cadastral areas of Trentino [41]. The thematic map has been generated by visual interpretation of a very high resolution orthophoto (20 cm), Google Maps, Maps Street View, Google Earth, and cartographic information.

There is no specific legend as per land cover information, but just the boundaries for the different cadastral parcels (as a shapefile). For the validation process, the areas corresponding to agriculture/crops are selected by means of the CLC map of 2018 in intersection with the boundaries offered by the Trentino region maps of 2017.

4) *Basilicata Region—33TXE Tile*: Geospatial data for the Basilicata region is published online since 2011 by Regionale dei Dati Spaziali della Regione Basilicata (RSDI) [42], [43]. The study area covers an extensive part of the southern Apennine mountains (9.995 km<sup>2</sup>) and it is the most mountainous region in the South of Italy. The area consists of a large number of small crop fields mainly sowable (especially wheat), which represent 46% of the total land. Potatoes and maize that are produced in the mountain areas. The available data focus on a portion of territory bounded by crop limits and elements of the land (ditches, drains, etc.), intended for both seasonal and annual agricultural activities. The information is provided as vector files at 1:5000 scale derived from photos. The information was integrated with auxiliary data from field detection and corresponds to the 2015 agrarian year. Despite this article focuses the attention on 2017 and 2018 agrarian years, we expect the information provided by the RSDI to be valid, since we expect the crop-field boundaries to be stable in such a time span.

### C. Validation Process and Metrics

Based on the four selected tiles, the validation was performed at regional level: 32TPQ tile—Emilia Romagna (22.446 km<sup>2</sup>); 32TPR tile—Veneto (18.264 km<sup>2</sup>); 32TPS tile—Trentino (13.619 km<sup>2</sup>); and 33TXE tile—Basilicata (9.995 km<sup>2</sup>). For each region, freely available land cover maps and cadastral maps, together with CORINE Land Cover map of 2018, were considered for validation of the spatio-temporal fusion step from a qualitative and quantitative perspective. However, available maps offer information about administrative parcel boundaries, but not about the way they are used. This results in reporting less crop fields, as administrative parcels often show multiple cultivations. Making use of the boundaries extracted from ground truth, the data are converted to a Boolean format (where 0 represents no crop field and 1 represents a crop field) for quantitative validation. Two metrics are considered: Jaccard index or intersection over union [44] and BF score [45]. Both indices range from [0, 1], where 0 indicates no agreement between the two maps, and 1 indicates complete agreement. Regarding the daily time series reconstruction, the MSE w.r.t. the linear original NDVI-SITS was considered for evaluation. Finally, the phenological parameters extraction were evaluated from a qualitative perspective only, since such information is not available.

## IV. EXPERIMENTAL RESULTS AND VALIDATION

The proposed method was applied over the whole Italy. Because of size and amount of details we do not report the resulting map in the article. Readers are referred to [30] to explore it. However, average results at Country level are reported and discussed. In order to better illustrate results, we focus the attention on the four tiles mentioned in the validation sub-section. Given the type of reference data for each tile, and space constrains, further

TABLE II  
COMPUTATIONAL TIME BASED ON 32TPQ TILE

Step	Time
Data Management/Loading	35 min
Agricultural areas map generation	2.5 h
Spatio-temporal fusion	9 min
Time series reconstruction	54 min
Phenological parameters	23 min
Total per single tile	~4.5 h
Total per 60 tiles (estimation)	270 h / 11.25 days

details about the MT vegetation maps and the phenological parameters map are shown for a portion of the Emilia-Romagna tile only. However, the results are representative for all the tiles.  $T_v$  was set to  $T_v = 5 \times 10^{-3}$  and the initial standard deviation value for the Gaussian kernel in the GRNN was set to 0.1. The generation of reliable agricultural areas map for 2017 and 2018 agrarian years was carried out based on [46]. The method requires between 3–5 images per year (per tile) to update a previously existing land cover map. The whole process took about 2.5 h per tile and per year in an Intel Core i7-7700 CPU running at 3.60 GHz with 32 GB of RAM. As the last step, S2 agricultural areas were characterized by first identifying single crop fields (using ten images) and then extracting phenological parameters using all the images in the S2-SITS [13]. Images with a cloud coverage higher than 75% were filtered out. The time to perform the agricultural areas characterization was about 1.48 h per tile and per year with 100–200 images per year. This time is a function of computational capacity, but also of the number of crop fields (that varies tile by tile).

### A. Average Results, Computational Time and Parameters Sensitivity for Italy

To assess the performance at Country level, we analyzed the number of crop fields per tile, MSE for the time series reconstruction step, computational time and parameters sensitivity over Italy. Fig. 6 shows the number of crop fields and MSE for the 60 tiles for 2017 and 2018 agrarian years. The number of crop fields varies across the tiles but tends to remain stable from one agrarian year to the other. Yet, the MSE is low for all the tiles and the two agrarian years, proving the robustness of the proposed method. For the computational time, we took as reference the 32TPQ tile being the one with the largest number of crop fields over Italy. Table II gives the computational times per each stage (excluding the download and preprocessing step that took about 15 days for all the data) at 32TPQ tile level and uses it to estimate an upper bound over the 60 tiles per agrarian year. The data management/loading step refers to the insertion of data inside python to be processed. The most computationally heavy steps were those of the agricultural areas map generation and the time series reconstruction. Yet, these times can be considered small compared to the amount of data. To process the Italian Country, in a single machine (see Section III-A for details), it took ~11.25 days.

To further understand the correlation between parameters of the proposed approach and the average variance for all the crop fields, parameter sensitivity analysis was carried out. The most important parameters, tolerance value ( $T_v$ ) and  $k$  factor, were

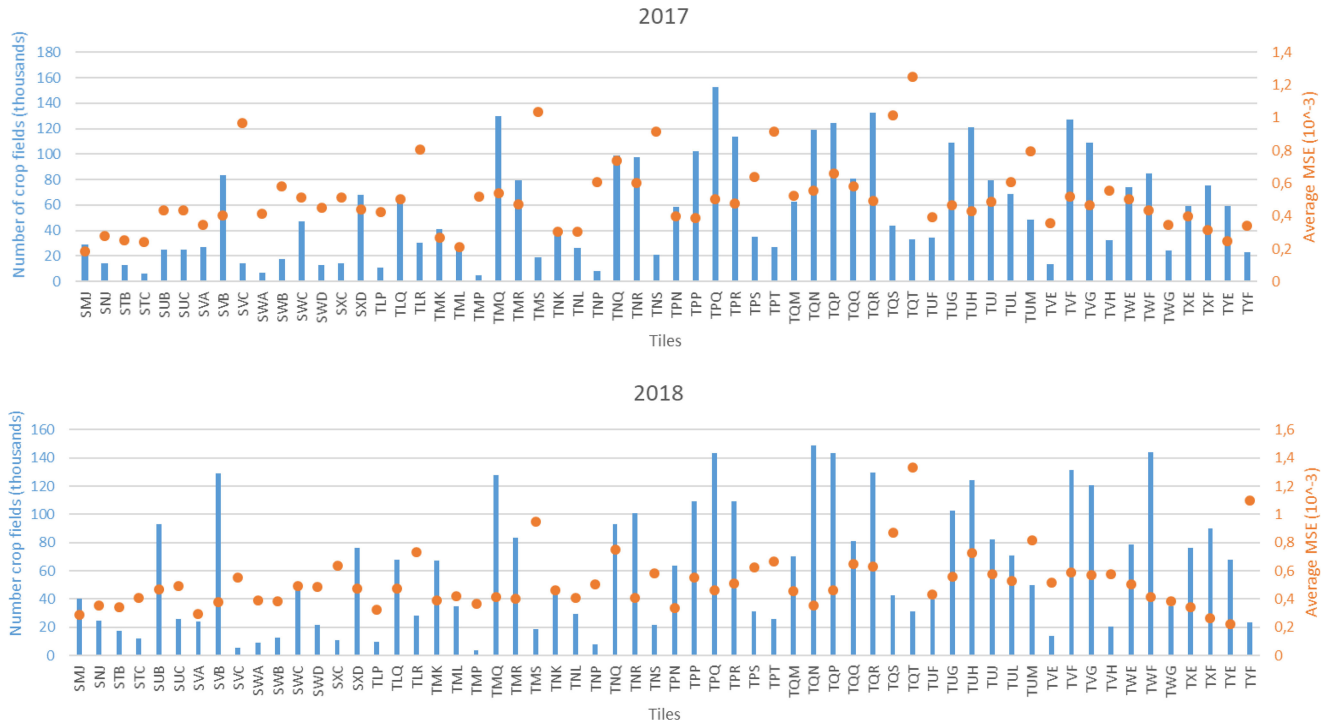


Fig. 6. Number of crop fields (thousands) and average MSE ( $10^{-3}$ ) for time series reconstruction step per tile and agrarian year.

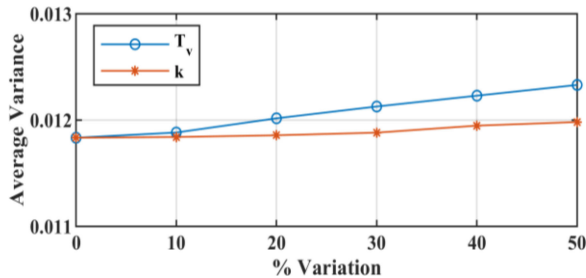


Fig. 7. Sensitivity analysis of  $T_v$  and  $k$  parameters with respect to average variance.

positively increased according to the magnitude in the range [10%, 50%] in steps of 10%, and the increment of average variance was observed [47]. Results are reported in terms of average over the 60 Italian tiles (see Fig. 7). It is clear that the average variance remains relatively stable as the  $T_v$  and  $k$  values increase, showing a high robustness of the proposed method.

#### A. Emilia-Romagna Region—32TPQ Tile

In order to prove the robustness of the proposed approach to MT crop field map in 2017 and 2018, Fig. 8 shows an example of a portion of the 32TPQ, where the evaluation is carried out by considering the variance inside each crop field. Under the assumption that the crop field is homogeneous, a correct detection implies small variance. The lower the variance, the better the detection of the crop field. According to Fig. 8, the variance ranges from [0, 0.05] and proves a reliable separation of crop fields in a robust way at both spatial and temporal levels.

TABLE III  
MEAN VARIANCE, JACCARD INDEX, AND BF SCORE FOR ALL THE CROP FIELDS FOUND IN 32TPQ TILE FOR 2017

Method	Mean Variance	Jaccard Index	BF score	# Crop Fields
Reference Data	0.0131	0.4644	0.6976	43194
Proposed Approach	0.0108			152627

In order to further prove the results, the variance, Jaccard index and BF score were calculated for all the crop fields in 32TPQ tile for both the proposed approach and the reference data (see Table III). One can see that the proposed approach behaves in a better way from the variance perspective. The number of crop fields detected by the proposed approach is more than three times the one reported by the reference map. As mentioned before, these results should be related to the way in which the reference map is built. The level of agreement between both maps is high, as per Jaccard index and BF score.

Once a reliable MT crop field map is obtained, a daily NDVI-SITS can be reconstructed for each crop field. Here, we compare the results obtained with the linear and upper-envelope methods. The reader is referred to [24] for further comparisons. Fig. 9 shows the NDVI-SITS reconstruction examples for two crop fields in the 32TPQ tile in 2017. On the bottom part of the plot, the MSE for the proposed approach along the year is also shown. The average MSE for 2017 over the entire tile is  $0.8 \times 10^{-3}$ , which is satisfactory. It should be noted that most of the errors correspond to those areas where the original NDVI trend is lower than the expected one. In other words, areas where atmospheric conditions alter the NDVI average trend. For some crop fields, these lower peaks are even larger, increasing the mean MSE.



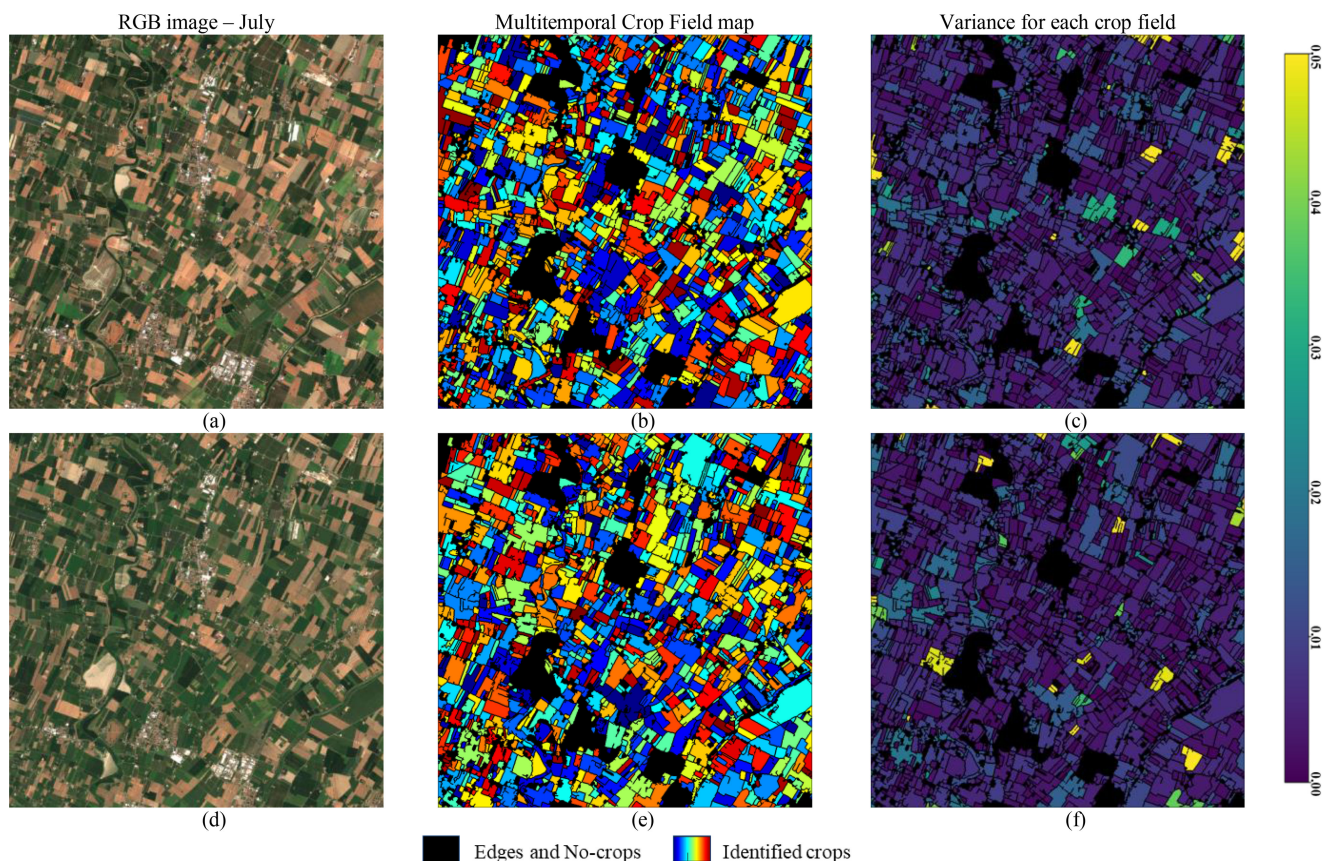


Fig. 8. Spatio-temporal fusion step results for a small portion ( $1000 \times 1000$  pixels) of Emilia Romagna region (tile 32TPQ) for year (b) 2017 and (e) 2018 agrarian years with evaluation of variance for each crop field (c) and (f), respectively.

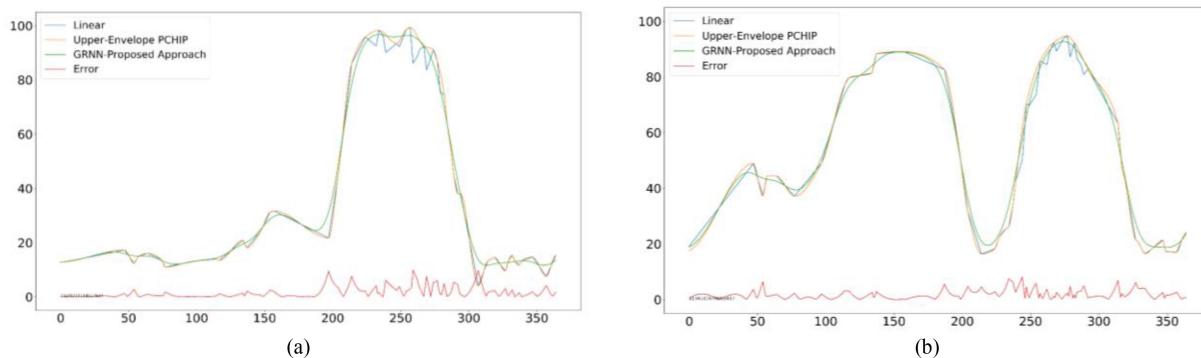


Fig. 9. NDVI-SITS reconstruction for three different methods in a crop field located in (a) Santa Vittoria and (b) Castelluccio for 2017.

However, looking at the whole result, it is clear that the proposed approach properly follows the NDVI-SITS over time.

Crop-type information from the reference map is used in order to validate the reliability of phenological parameters extraction (e.g., beginning, middle, and end of season). We expect to have a similar behavior (in time) for crop fields belonging to the same type of crop. This is the case in Fig. 10, where crop fields corresponding to vineyard in the reference map have been masked and three phenological parameters have been extracted. Color coding varies from blue to red as the year progresses and refers to the week/month in which events (e.g., the beginning of season) happened.

### B. Veneto Region—32TPR Tile

Similar to the Emilia-Romagna region, the variance, Jaccard index and BF score for all the crop fields in the 32TPR tile were calculated. Results can be seen in Table IV, where the variances for reference data and the proposed approach are quite similar. As expected, the number of crop fields is nearly seven times more than reference data. The level of agreement between both maps is high, as per Jaccard index and BF score.

In order to further prove the correctness of the proposed approach, a small portion of the entire tile (located in Negora-Veneto) was selected. Fig. 11 shows the RGB, reference map and MT crop field map from the proposed approach. Comparing the

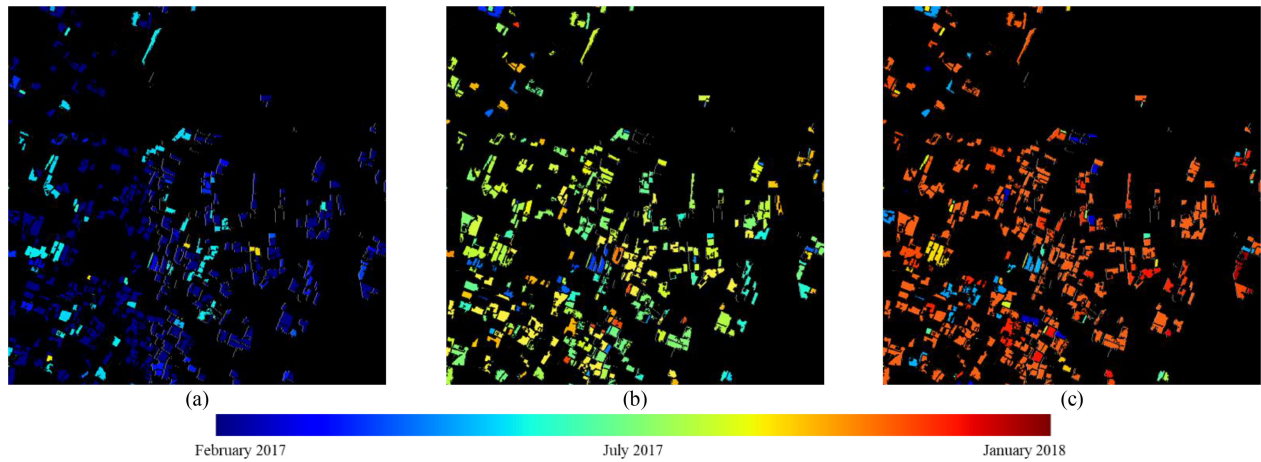


Fig. 10. Phenological parameter maps for vineyards in tile 32TPQ (Emilia Romagna region) during 2017 agrarian year. (a) Beginning of season. (b) Middle of season. (c) End of season (black color corresponds to non-agricultural areas).

TABLE IV  
MEAN VARIANCE, JACCARD INDEX AND BF SCORE FOR ALL THE CROP FIELDS FOUND IN 32TPR TILE FOR 2017

Method	Mean Variance	Jaccard Index	BF score	# Crop Fields
Reference Data	0,0100	0,5072	0,6602	15966
Proposed Approach	0,0110			113764

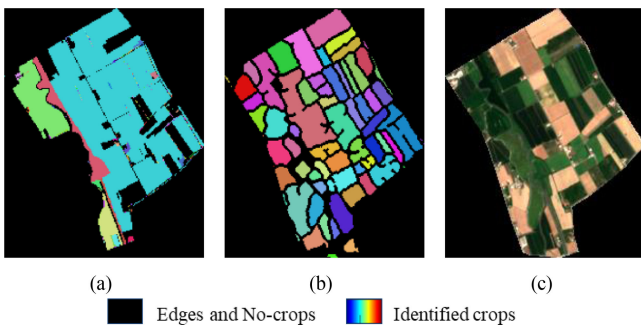


Fig. 11. MT crop field map for (a) reference map and (b) proposed approach, together with (c) an RGB composition for an area located in Negora-Veneto.

maps to the RGB image, it is clear how the proposed approach correctly detects and separates the different crop fields, w.r.t. the reference map. In Fig. 11, only a rather small area of the entire tile is shown, which allows to understand why there is such a big difference in the number of detected crop fields and that this number is more coherent with the true color composition in Fig. 11(c) rather than reference map in Fig. 11(a).

Analyzing the variance of the big light blue area in Fig. 11(a) over time, it is also possible to see that the reference map has incorrectly mapped the crop fields. Fig. 12 shows the evolution of the variance (for the original acquisition dates) for a crop field over the 2017 agrarian year for both the reference and the proposed approach maps. It appears how the variance remains stable along the year for the proposed approach, whereas it shows a large variation for the reference map, implying that the field includes contributions from non-homogeneous crops.

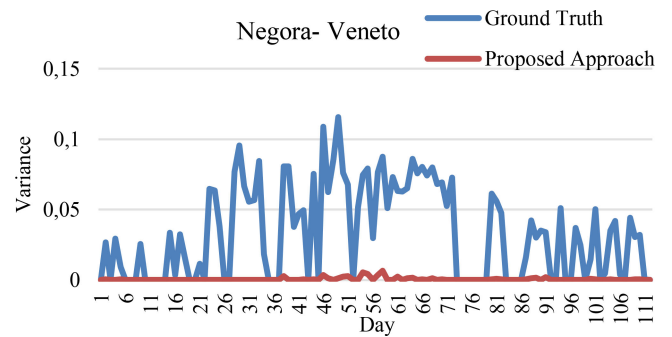


Fig. 12. Variance temporal plot for a single crop field in an area located in Negore-Veneto for 2017 agrarian year.

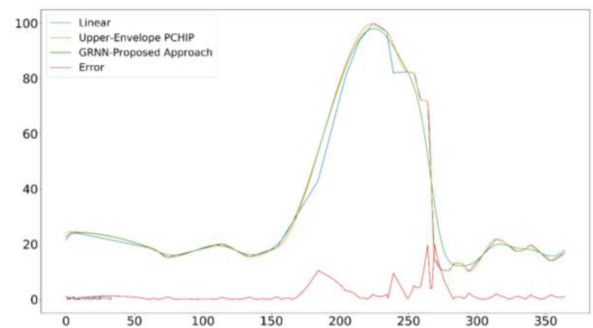


Fig. 13. NDVI-SITS reconstruction for three different methods in a crop field located in Negora for 2017.

Regarding the NDVI-SITS, the proposed approach is compared to the linear reconstruction. Fig. 13 compares results for one area in the Veneto region, as well as the MSE error for the proposed approach. The mean MSE for all the crop fields in the entire tile is  $0.7 \times 10^{-3}$ . This value is low and similar to that of the Emilia-Romagna region, showing how the reconstruction is correlated to the good crop field detection/separation. The results for the phenological parameters are similar to those of the Emilia-Romagna region, and thus not reported.



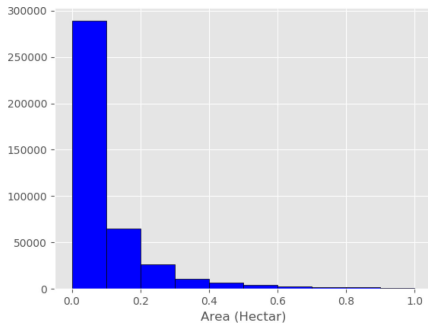


Fig. 14. Area histogram for all the crop fields in the entire 32TPS tile.

TABLE V  
MEAN VARIANCE, JACCARD INDEX, AND BF SCORE FOR ALL THE CROP FIELDS FOUND IN 32TPS TILE FOR 2017

Method	Mean Variance	Jaccard Index	BF score	# Crop Fields
Reference Data	0.0050	0.4987	0.6677	228411
Proposed Approach	0.0095	0.4987	0.6677	35424

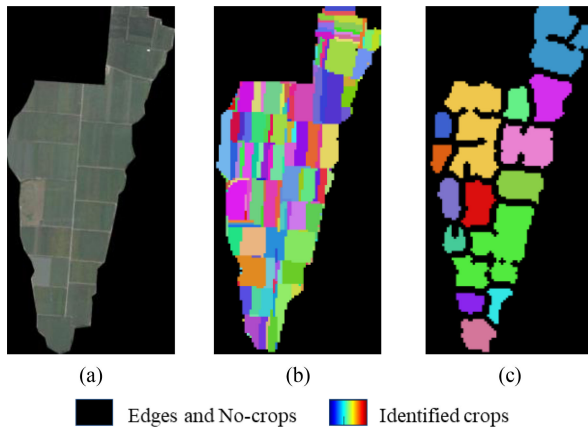


Fig. 15. MT crop field map for (b) Reference map and (c) proposed approach, together with an (a) RGB composition for an area located in Mollaro–Trentino.

### C. Trentino Alto Adige Region—32TPS Tile

Trentino is a region with a remarkable number of permanent vineyards and apple trees, and small crop fields. Indeed, most of the crop fields are smaller than 1ha, as shown in the histogram in Fig. 14. Only around 4000 crop fields (out of 228411) are bigger than that. Therefore, this is a challenging area to test the robustness of the proposed approach, since three out of four assumptions are not satisfied.

As done for the 32TPQ and 32TPR tiles, the variance, Jaccard index and BF score were calculated for every crop field along the 2017 agrarian year, both for the reference map and the proposed approach. Results can be seen in Table V. Although the conditions for the proposed approach to properly work are not satisfied, both the reference map and the proposed approach show comparable variance values. The level of agreement between both maps is further corroborated by Jaccard index and BF score. The number of crop fields found by the proposed approach is 6 times less than the reference map. In Figs. 15 and 16, we picked a small area for qualitative comparison.

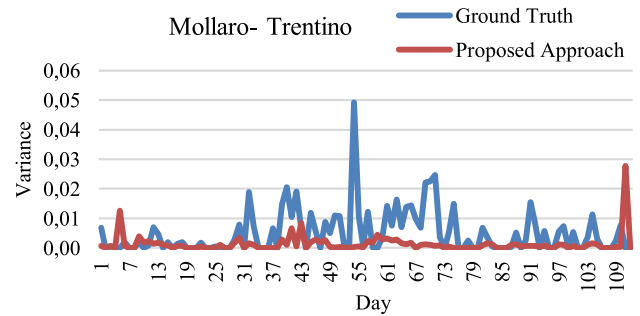


Fig. 16. Variance temporal plot for a single crop field in an area located in Mollaro–Trentino for 2017 agrarian year.

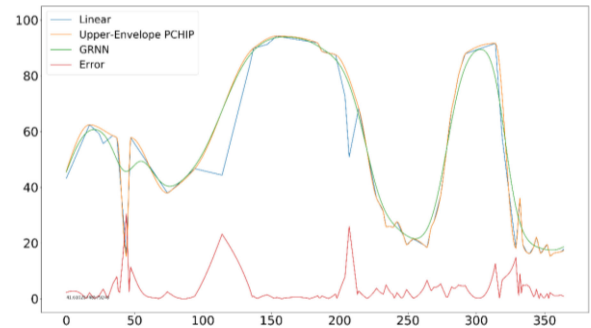


Fig. 17. NDVI-SITS reconstruction for three different methods in a crop field located in Valtina–Walten for 2017.

While the MT crop field map groups several individual crop fields [see Fig. 15(a) versus Fig. 15(c)], the variance temporal plot for a single crop shown in Fig. 16 demonstrates the reliability of the proposed approach. In fact, the variance along time for the proposed approach varies less than the one of the reference map. This is because adjacent fields are managed in the same way.

Regarding the NDVI-SITS, the proposed approach is compared to the original linear reconstruction. Fig. 17 shows the comparison for one area located inside the Trentino Alto Adige region, as well as the MSE for the proposed approach. The crop fields mean MSE is  $0.6 \times 10^{-3}$ . This value is low, and similar to that of the other tiles, proving the reliability of MT crop field separation. Fig. 17 shows how around day 50, there is a rather low peak of the standard NDVI trend. Such value is usually confused by any method as an actual peak, but the proposed time series reconstruction method is able to better deal with it, showing a smoother NDVI-SITS trend. The results for the phenological parameters cannot be compared to any land cover map of the area, since the reference map does not provide information on the crop types. Nevertheless, they can be considered reliable based on the phenological evolution of the type of crops that are traditionally cultivated in the area (i.e., vineyards and apples mostly).

### D. Basilicata Region—33TXE Tile

Similar to the Trentino region, Basilicata contains a large amount of small crop fields, but given climate differences they show different crop types and thus phenological behaviors. As shown in the histogram in Fig. 18, a huge amount of crop fields

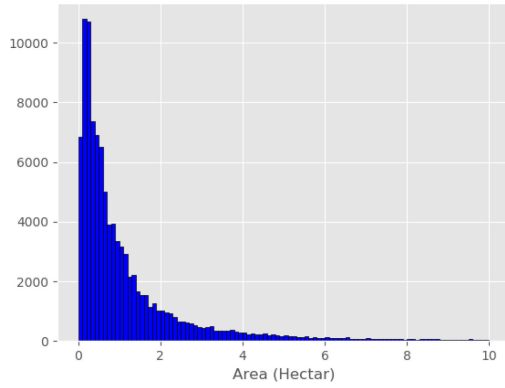


Fig. 18. Area histogram for all the crop fields in the entire 33TXE tile.

TABLE VI  
MEAN VARIANCE, JACCARD INDEX, AND BF SCORE FOR ALL THE CROP FIELDS FOUND IN 33TXE TILE FOR 2017

Method	Mean Variance	Jaccard Index	BF score	# Crop Fields
Reference Data	0.0091			103149
Proposed Approach	0.0118	0.4511	0.7088	59557

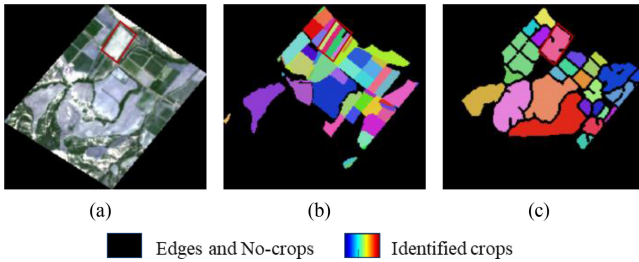


Fig. 19. MT crop field map for (b) reference map and (c) proposed approach, together with an (a) RGB composition for an area located in Ponte Masone - Basilicata.

has an area smaller than 1 ha and about 89% equal or smaller than 3 ha, making the analysis challenging (according to the method working conditions).

Similar to the other validation tiles, we calculated the variance for every single field along the whole 2017 agrarian year, both for the ground truth and the proposed approach. Table VI gives that the proposed approach has a reliable performance compared to the ground truth in terms of variance parameters.

On the one side, the crop field map generated by the proposed method can properly define the borders for large crop fields (more than 1 ha—Fig. 19). On the other side, let us observe a portion of the reference map where crop fields are small. In red box [see Fig. 19(a)] the reference map shows four crop fields, whereas the proposed approach detects a single crop field. As can be seen from the true color composite image, this area shows to be homogeneous. In order to prove the correctness of the proposed approach outcome, the average variance for the four crop fields is compared to that of each parcel in the reference map (see Fig. 20). Fig. 20 shows that the variance of the four parcel and the one of the field by the proposed method are very close to each other over the entire agrarian year. Accordingly,

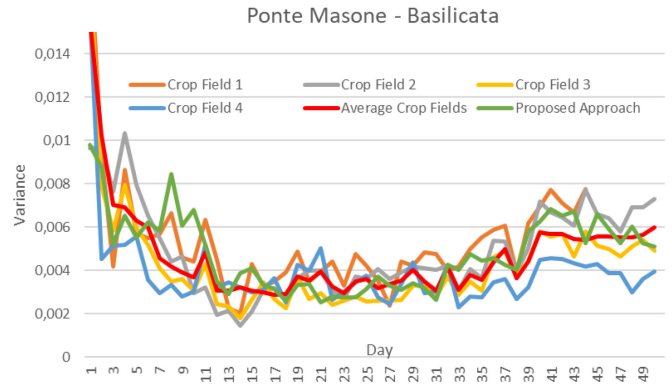


Fig. 20. Variance temporal plot for a single crop field in an area located in Ponte Masone-Basilicata for 2017 agrarian year.

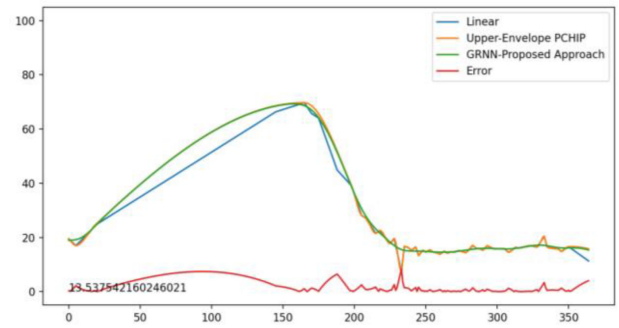


Fig. 21. NDVI-SITS reconstruction for three different methods in a crop field located in Ponte Masone-Basilicata for 2017.

the four parcels are likely to be cultivated in the same way and the method detects them as one single crop field.

Regarding the NDVI-SITS, the proposed approach is compared to the linear reconstruction. Fig. 21 compares results for one area in the Basilicata region, as well as the MSE error for the proposed approach. The mean MSE for all the crop fields in the entire tile is  $0.4 \times 10^{-3}$ . This value is low, and similar to that of the other tiles, proving the reliability of MT crop field separation. Fig. 21 shows how around day 230, there is a low peak of the standard NDVI trend that the proposed time series reconstruction method is able to better deal with. The results for the phenological parameters are similar to those of the Emilia-Romagna region, and thus not reported.

## V. DISCUSSION

This article aimed to give answer to two research questions: how to handle big amount of data with particular attention to download and preprocessing of S2-SITS; and how to perform multi-temporal fine characterization of crop fields accounting for the strong variability in size and phenological behaviors when mapping at large scale.

In order to handle big amounts of data, the proposed approach guides users from the beginning to the end in the process of automatically downloading, preprocessing and analyzing data, while accounting for possible critical issues arising while handling big data. Some of them are related to download failures, restrictions parallel data download, lack of fully preprocessed data and



errors in the preprocessing steps resulting in incomplete final products. It also considers computational burden. When dealing with Italian Country, 12.97 TB of data have been downloaded and pre-processed in about 15 days. Given the amount of data the time can be considered short. However, it might strongly vary according to parameters (like internet connection speed or stability) being out of the user control. In Table II, computational times for the most complex tile (32TPQ) are detailed showing that the proposed approach can work in real time by completing the analysis of a single tile in 4.5 h.

A detailed approach to perform multitemporal characterization of crop fields has also been presented that further proves the reliability of the entire framework. Results are presented for four tiles being representative of and distributed across Italy (see Fig. 5). Tables III–VI prove the capability of the spatio-temporal fusion step to properly identify and separate fields that have been cultivated at least once over the agrarian year. The statistical analysis of mean variance and the Jaccard index prove the level of agreement between results and reference maps. In this, it is important to recall that reference maps were built by different entities across Italy for different tiles, paying attention to parcel level information rather than subparcel level usage. Because of this, it was expected that the proposed approach would identify a larger number of crop fields per tile. This is not to be understood as something that penalizes the proposed approach. In fact, Figs. 6, 8, 11, 15, and 19 clearly show how the proposed approach better follows the situation on the ground provided by the RGB images. The method demonstrated to be effective even for the trentino alto adige (32TPS) and Basilicata (33TXE) tiles, where the crop field areas are so small that not all the working hypothesis of the proposed approach are satisfied. Yet, the proposed approach is able to detect the crop fields and map them in a reliable way (according to the mean variance). A further confirmation of effectiveness comes from the analysis of phenological parameters of crop fields with the same cultivation. Fig. 10 shows an example for three vineyards phenological parameters. As can be observed, they behave similarly along time for all the vineyards. The homogeneity confirms the accurate mapping of fields. Similar results were obtained over Italy and for the two considered years. The S2-SITS reconstruction step performance was compared to the linear and upper-envelope methods following the approach in [24]. Figs. 9, 13, 17, and 21 show the comparisons for different crop fields in the corresponding validation tiles. It is clear from the plots and the MSE (with a factor of  $10^{-3}$ ) that the proposed approach properly models the phenological behavior of the crops, while keeping a low error in the process.

## VI. CONCLUSION

In this article, an automatic approach to precise mapping and monitoring of small agricultural fields at large-scale based on S2 SITS has been presented. The proposed approach has been tailored to the specific properties of S2 images. It has been developed to exploit high spatial resolution multitemporal images of S2-SITS and to deal with the download and preprocessing of data. In this article, the state of the art was analyzed in order to identify important and strategic approaches and challenges and ways to effectively address them. The proposed approach: effectively handles big amount of data with particular attention

to download and preprocessing of S2-SITS in an automatic way; characterizes agricultural areas by exploiting MT information to effectively separate small crop fields from each other in an unsupervised way at large-scale; deals with irregularities in the data due to high variability while working at large-scale and; and is robust to space and time variance (across the Country and the years). Crop fields separation relies on an effective spatio-temporal fusion that considers phenological behavior of the vegetation in space and time. Moreover, to deal with irregular data, an ad-hoc nonparametric and adaptive regression model was tuned that automatically reconstructs daily temporal signatures at crop field level.

Results have been obtained on real S2 data of Italy for 2017 and 2018 agrarian years. Specific examples of precise mapping have been shown for different test sites, i.e., 32TPQ, 32TPR, 32TPS, and 33TXE tiles, representative of different land covers in Italy. The qualitative and quantitative validation analysis demonstrated the effectiveness and robustness of the proposed approach while working at large-scale and dealing with high temporal, spatial, and spectral variability, as well as with small crop fields. Future developments deal with the tuning on other Countries by considering additional variables like for example climate regions. Data are available at [30].

## ACKNOWLEDGMENT

The authors would like to thank D. Carcereri for his contribution to test part of the method.

## REFERENCES

- [1] F. Bovolo, L. Bruzzone, and Y. T. Solano-Correa, "Multitemporal analysis of remotely sensed image data," in *Comprehensive Remote Sensing*, S. Liang, Ed., Oxford, U.K.: Elsevier, 2018, pp. 156–185.
- [2] Home page - CREODIAS. Accessed: Aug. 2021. [Online]. Available: <https://creodias.eu/>
- [3] Y. Ma, T. He, A. Li, and S. Li, "Evaluation and intercomparison of topographic correction methods based on landsat images and simulated data," *Remote Sens.*, vol. 13, no. 20, Jan. 2021, Art. no. 4120.
- [4] D. Frantz, A. Röder, M. Stellmes, and J. Hill, "An operational radiometric landsat preprocessing framework for large-area time series applications," *IEEE Trans. Geosci. Remote Sens.*, vol. 54, no. 7, pp. 3928–3943, Jul. 2016, doi: [10.1109/TGRS.2016.2530856](https://doi.org/10.1109/TGRS.2016.2530856).
- [5] A. Lewis *et al.*, "The Australian geoscience data cube — Foundations and lessons learned," *Remote Sens. Environ.*, vol. 202, pp. 276–292, Dec. 2017.
- [6] C. Persello, V. A. Tolpekin, J. R. Bergado, and R. A. de By, "Delineation of agricultural fields in smallholder farms from satellite images using fully convolutional networks and combinatorial grouping," *Remote Sens. Environ.*, vol. 231, Sep. 2019, Art. no. 111253.
- [7] K. M. Masoud, C. Persello, and V. A. Tolpekin, "Delineation of agricultural field boundaries from Sentinel-2 images using a novel super-resolution contour detector based on fully convolutional networks," *Remote Sens.*, vol. 12, no. 1, Jan. 2020.
- [8] F. Waldner *et al.*, "Detect, consolidate, delineate: Scalable mapping of field boundaries using satellite images," *Remote Sens.*, vol. 13, no. 11, Jan. 2021.
- [9] B. D. Wardlow and S. L. Egbert, "Large-area crop mapping using time-series MODIS 250 m NDVI data: An assessment for the U.S. central great plains," *Remote Sens. Environ.*, vol. 112, no. 3, pp. 1096–1116, Mar. 2008.
- [10] J. O'Connell, U. Bradter, and T. G. Benton, "Wide-area mapping of small-scale features in agricultural landscapes using airborne remote sensing," *ISPRS J. Photogramm. Remote Sens.*, vol. 109, pp. 165–177, Nov. 2015.
- [11] Y. Hamrouni, É. Paillassa, V. Chéret, C. Monteil, and D. Sheeren, "From local to global: A transfer learning-based approach for mapping poplar plantations at large scale," in *Proc. Mediterranean Middle-East Geosci. Remote Sens. Symp.*, Mar. 2020, pp. 242–245.

- [12] H. I. Fawaz, G. Forestier, J. Weber, L. Idoumghar, and P.-A. Muller, "Deep learning for time series classification: A review," Sep. 2018. [Online]. Available: <http://arxiv.org/abs/1809.04356>
- [13] L. Ma, Y. Liu, X. Zhang, Y. Ye, G. Yin, and B. A. Johnson, "Deep learning in remote sensing applications: A meta-analysis and review," *ISPRS J. Photogrammetry Remote Sens.*, vol. 152, pp. 166–177, Jun. 2019.
- [14] M. E. A. Larabi, S. Chaib, B. Khadija, K. Hasni, and M. A. Bouhlala, "High-resolution optical remote sensing imagery change detection through deep transfer learning," *J. Appl. Remote Sens.*, vol. 13, no. 4, Nov. 2019, Art. no. 046512.
- [15] Google Earth Engine. Accessed: Aug. 24, 2020 [Online]. Available: <https://earthengine.google.com/>
- [16] DARPA, "XDATA." Accessed: Jan. 23, 2022. [Online]. Available: <https://www.darpa.mil/program/xdata>
- [17] Earth observing system data and information system (EOSDIS)|Earthdata. Accessed: Feb. 8, 2021. [Online]. Available: <https://earthdata.nasa.gov/eosdis/>
- [18] M. Hajirahimova and A. S. Aliyeva, "Big Data initiatives of developed countries," *Problem Inf. Soc.*, vol. 8, no. 1, pp. 10–19, Jan. 2017, doi: [10.25045/jpis.v08.i1.02](https://doi.org/10.25045/jpis.v08.i1.02).
- [19] Y. Huang, Z. Chen, T. Yu, X. Huang, and X. Gu, "Agricultural remote sensing Big Data: Management and applications," *J. Integr. Agriculture*, vol. 17, no. 9, pp. 1915–1931, Sep. 2018.
- [20] Google Earth Engine, "Sentinel-2 MSI: Multispectral instrument, Level-2A | Earth Engine data catalog," *Google Developers*. Accessed: Jan. 23, 2022. [Online]. Available: [https://developers.google.com/earth-engine/datasets/catalog/COPERNICUS\\_S2\\_SR](https://developers.google.com/earth-engine/datasets/catalog/COPERNICUS_S2_SR)
- [21] L. Li, M. A. Friedl, Q. Xin, J. Gray, Y. Pan, and S. Frolking, "Mapping crop cycles in China using MODIS-EVI time series," *Remote Sens.*, vol. 6, no. 3, pp. 2473–2493, Mar. 2014.
- [22] L. Yan and D. P. Roy, "Automated crop field extraction from multi-temporal web enabled landsat data," *Remote Sens. Environ.*, vol. 144, pp. 42–64, Mar. 2014.
- [23] M. Turker and E. H. Kok, "Field-based sub-boundary extraction from remote sensing imagery using perceptual grouping," *ISPRS J. Photogramm. Remote Sens.*, vol. 79, pp. 106–121, May 2013.
- [24] Y. T. Solano-Correa, F. Bovolo, L. Bruzzone, and D. Fernández-Prieto, "A method for the analysis of small crop fields in sentinel-2 dense time series," *IEEE Trans. Geosci. Remote Sens.*, vol. 58, no. 3, pp. 2150–2164, Mar. 2020.
- [25] L. Bruzzone, F. Bovolo, C. Paris, Y. T. Solano-Correa, M. Zanetti, and D. Fernández-Prieto, "Analysis of multitemporal sentinel-2 images in the framework of the ESA scientific exploitation of operational missions," in *Proc. 9th Int. Workshop Anal. Multitemporal Remote Sens. Images (MultiTemp)*, Jun. 2017, pp. 1–4.
- [26] Y. T. Solano-Correa, F. Bovolo, L. Bruzzone, and D. Fernández-Prieto, "Spatio-temporal evolution of crop fields in sentinel-2 satellite image time series," in *Proc. 9th Int. Workshop Anal. Multitemporal Remote Sens. Images (MultiTemp)*, Jun. 2017, pp. 1–4.
- [27] Y. T. Solano-Correa, F. Bovolo, L. Bruzzone, and D. Fernández-Prieto, "Automatic derivation of cropland phenological parameters by adaptive non-parametric regression of sentinel-2 NDVI time series," in *Proc. IGARSS*, Jul. 2018, pp. 1946–1949.
- [28] L. Yan and D. P. Roy, "Conterminous United States crop field size quantification from multi-temporal landsat data," *Remote Sens. Environ.*, vol. 172, pp. 67–86, Jan. 2016.
- [29] P. Defourny *et al.*, "Near real-time agriculture monitoring at national scale at parcel resolution: Performance assessment of the Sen2-agri automated system in various cropping systems around the world," *Remote Sens. Environ.*, vol. 221, pp. 551–568, Feb. 2019.
- [30] ESA SEOM-S2-4Sci land and water multitemporal analysis (MTA) | RSLab. Oct. 2018. Accessed: Oct. 29, 2018. [Online]. Available: <http://rslab.disi.unitn.it/projects/mta/>
- [31] SentinelSat — SentinelSat 0.13 documentation. Accessed: Jan. 13, 2020. [Online]. Available: <https://sentinelat.readthedocs.io/en/stable/>
- [32] Open access hub. Accessed: Jun. 17, 2021. [Online]. Available: <https://scihub.copernicus.eu/userguide/>
- [33] G. Doxani *et al.*, "Atmospheric correction inter-comparison exercise," *Remote Sens.*, vol. 10, no. 2, Feb. 2018.
- [34] V. Zekoll *et al.*, "Comparison of masking algorithms for sentinel-2 imagery," *Remote Sens.*, vol. 13, no. 1, Jan. 2021.
- [35] E. ESA, "ESA - Sen2Cor configuration and user manual," Dec. 2017. Accessed: Jan. 2, 2018. [Online]. Available: <http://step.esa.int/main/third-party-plugins-2/sen2cor/>
- [36] S.-2 ESA, "Spatial - resolutions - sentinel-2 MSI - user guides - sentinel online - sentinel online." Accessed: Aug. 4, 2021. [Online]. Available: <https://sentinels.copernicus.eu/web/sentinel/user-guides/sentinel-2-msi/resolutions/spatial>
- [37] D. F. Specht, "A general regression neural network," *IEEE Trans. Neural Netw.*, vol. 2, no. 6, pp. 568–576, Nov. 1991, doi: [10.1109/72.97934](https://doi.org/10.1109/72.97934).
- [38] "Python | pandas dataframe.groupby," GeeksforGeeks, Noida, India, Nov. 2018. Accessed: Jan. 13, 2020. [Online]. Available: <https://www.geeksforgeeks.org/python-pandas-dataframe-groupby/>
- [39] Emilia-Romagna, "Arpa emilia-romagna," *Arpa Emilia-Romagna*. Accessed: Apr. 5, 2021. [Online]. Available: <https://www.arp.ae.it/it>
- [40] Agenzia Veneta per i Pagamenti, "Usò del suolo - avepa." Accessed: Apr. 5, 2021. [Online]. Available: <https://www.avepa.it/uso-suolo>
- [41] Provincia Autonoma di Trento, "Carte della provincia autonoma di trento." Accessed: Apr. 5, 2021. [Online]. Available: [https://wgtis.provincia.tn.it/wgt/?lang=it&topic=1&bgLayer=sfondo&layers=ammcom&layers\\_visibility=false&catalogNodes=1](https://wgtis.provincia.tn.it/wgt/?lang=it&topic=1&bgLayer=sfondo&layers=ammcom&layers_visibility=false&catalogNodes=1)
- [42] RSDI, "RSDI," Mar. 2015. Accessed: Jan. 23, 2022. [Online]. Available: <http://rsdi.regione.basilicata.it/>
- [43] E. C.-J. R. Centre, "INSPIRE geoportal." Accessed: Jan. 23, 2022. [Online]. Available: <http://inspire-geoportal.ec.europa.eu/>
- [44] R. Real and J. M. Vargas, "Probabilistic basis of Jaccard's index of similarity | systematic biology | Oxford academic," *Systematic Biol.*, vol. 45, no. 3, pp. 380–385, Sep. 1996.
- [45] G. Csürka, D. Larlus, and F. Perronnin, "What is a good evaluation measure for semantic segmentation?," in *Proc. Brit. Mach. Vis. Conf.*, 2013, pp. 32.1–32.11.
- [46] C. Paris, L. Bruzzone, and D. Fernández-Prieto, "A novel approach to the unsupervised update of land-cover maps by classification of time series of multispectral images," *IEEE Trans. Geosci. Remote Sens.*, vol. 57, no. 7, pp. 4259–4277, Jul. 2019.
- [47] J. Zhang and J. Li, "A comparative study between infinite slope model and Bishop's method for the shallow slope stability evaluation," *Eur. J. Environ. Civil Eng.*, vol. 25, no. 8, pp. 1503–1520, Jul. 2021.



**Yady Tatiana Solano-Correa** (Member, IEEE) received the B.S. degree in physics engineering (Hons.) from the University of Cauca, Cauca, Colombia, in 2011, and the Ph.D. (*magna cum laude*) degree in communication and information technologies from the Department of Information Engineering and Computer Science, University of Trento, Trento, Italy, in 2018.

From 2009 to 2013, she was a Researcher for the research groups: Optics and Laser Group and Environmental Studies Group. From 2013 to 2020, she was a Researcher with the Remote Sensing for Digital Earth unit, FBK, Trento, Italy and a member of the RSLab with the University of Trento. She is currently an Assistant Professor with the University of Cauca. She works, and has worked, within the context of several projects with focus on analyzing information for climate change, water security and developing advanced change detection techniques for optical satellite time series data. Among them: RICCLISA—Interinstitutional network of climate change and food security, Colombia. Funded, financed by the Colombian administrative department of Science, Technology and Innovation – COLCIENCIAS; SEOM—Scientific Exploitation of Operational Missions—S2-4Sci Land and Water—Multitemporal Analysis. Funded, financed by European Space Agency, CCI+ HR LC—High Resolution Landcover Essential Climate Variable. Funded, financed by European Space Agency and Water Security and Sustainable Development Hub. Funded, financed by Global Challenges Research Fund and U.K. Research and Innovation. Her research interests include remote sensing environmental applications, change detection, both on medium resolution multispectral images, including Landsat and Sentinel-2 and very high resolution images, multitemporal analysis of short and long-time series, multisensor multitemporal image preprocessing and information extraction, pattern recognition, and image classification.

Dr. Solano-Correa is a Referee for the IEEE TRANSACTIONS ON GEOSCIENCE AND REMOTE SENSING, IEEE JOURNAL OF SELECTED TOPICS IN APPLIED EARTH OBSERVATIONS AND REMOTE SENSING and IEEE GEOSCIENCE AND REMOTE SENSING LETTERS journals. She was the recipient of the Best Student Oral Presentation Award at the MultiTemp 2017 Conference held in June 2017 in Bruges, Belgium and the best three Ph.D. thesis presented in 2018–2019 in the area of Geoscience and Remote Sensing, in Italy.



**Khaterah Meshkini** (Student Member, IEEE) received the bachelor's degree in electrical engineering from Zanjan University, Zanjan, Iran, in 2013, and the master's degree in telecommunication engineering from Science and Research University, Tehran, Iran, in 2016. She is currently working toward the Ph.D. degree with the Remote Sensing Laboratory, Department of Information and Communication Technologies, University of Trento and the Remote Sensing for Digital Earth Unit, Fondazione Bruno Kessler, Trento, Italy.

She has been involved in some projects for developing advanced methods in change detection of high resolution optical satellite images for climate change analysis, such as SEOM—Scientific Exploitation of Operational Missions—S2-4Sci Land and Water—Multitemporal Analysis. Funded, financed by European Space Agency in which she conducted the validation stage in the quality of the change detection products, and CCI+—High Resolution Landcover Climate Change Initiative—funded by ESA in which she is developing new methods to detect land cover changes in different areas in the world. Her research interests include remote sensing image processing, multispectral satellite image time series analysis, change detection in medium resolution, including Landsat and Sentinel-2 and very high resolution images, deep neural network for multitemporal satellite image processing, information extraction, image classification, and pattern recognition.



**Francesca Bovolo** (Senior Member, IEEE) received the Laurea (B.S.) degree, the Laurea Specialistica (M.S.) degree (*summa cum laude*) in telecommunication engineering, and the Ph.D. degree in communication and information technologies from the University of Trento, Trento, Italy, in 2001, 2003, and 2006, respectively.

She was a Research Fellow with the University of Trento, until 2013. She is currently the Founder and the Head of Remote Sensing for Digital Earth Unit, Fondazione Bruno Kessler, Trento, Italy, and a member of the Remote Sensing Laboratory, Trento, Italy. She is one of the Co-Investigators of the Radar for Icy Moon Exploration instrument of the European Space Agency Jupiter Icy Moons Explorer and member of the science study team of the EnVision mission to Venus. She conducts research on these topics within the context of several national and international projects. Her research interests include remote-sensing image processing, multitemporal remote sensing image analysis, change detection in multispectral, hyperspectral, and synthetic aperture radar images and very high-resolution images, time series analysis, content-based time series retrieval, domain adaptation, and Light Detection and Ranging and radar sounders.

Dr. Bovolo is a Member of the program and scientific committee of several international conferences and workshops. She was the recipient of the First Place in the Student Prize Paper Competition of the 2006 IEEE International Geoscience and Remote Sensing Symposium (Denver, 2006). She was the Technical Chair of the Sixth International Workshop on the Analysis of Multitemporal Remote-Sensing Images (MultiTemp 2011, and 2019). She has been a Co-Chair of the SPIE International Conference on Signal and Image Processing for Remote Sensing since 2014. She is the Publication Chair for the International Geoscience and Remote Sensing Symposium in 2015. She has been an Associate Editor for the IEEE JOURNAL OF SELECTED TOPICS IN APPLIED EARTH OBSERVATIONS AND REMOTE SENSING since 2011 and the Guest Editor of the Special Issue on Analysis of Multitemporal Remote Sensing Data of the IEEE TRANSACTIONS ON GEOSCIENCE AND REMOTE SENSING. She is a referee for several international journals.



**Lorenzo Bruzzone** (Fellow, IEEE) received the Laurea (M.S.) degree in electronic engineering (*summa cum laude*) and the Ph.D. degree in telecommunications from the University of Genoa, Genoa, Italy, in 1993 and 1998, respectively.

He is currently a Full Professor of telecommunications with the University of Trento, Italy, where he teaches remote sensing, radar, and digital communications. He is the Founder and Director of the Remote Sensing Laboratory, Department of Information Engineering and Computer Science, University of

Trento, Trento, Italy. He promotes and supervises research on these topics within the frameworks of many national and international projects. He is the Principal Investigator of many research projects. Among the others, he is currently the Principal Investigator of the *Radar for icy Moon exploration* instrument in the framework of the *JUPITER ICY MOONS EXPLORER* mission of the European Space Agency and the Science Lead for the *High Resolution Land Cover* project in the framework of the Climate Change Initiative of ESA. He has authored or coauthored 294 scientific papers in referred international journals, including 221 in IEEE journal, more than 340 papers in conference proceedings, and 22 book chapters. He is an Editor/Co-Editor of 18 books/conference proceedings and one scientific book. His papers are highly cited, as proven from the total number of citations (more than 41000) and the value of the h-index (93) (source: Google Scholar). He was invited as a Keynote Speaker in more than 40 international conferences and workshops. Since 2009, he has been a Member of the Administrative Committee of the IEEE Geoscience and Remote Sensing Society (GRSS), where since 2019, he has been the Vice-President for Professional Activities. His current research interests include remote sensing, radar and SAR, signal processing, machine learning, and pattern recognition.

Dr. Bruzzone was the recipient of first prize in the Student Prize Paper Competition of the 1998 IEEE International Geoscience and Remote Sensing Symposium, Seattle, WA, USA, July 1998 and many international and national honors and awards, including the recent *IEEE GRSS 2015 Outstanding Service Award*, 2017 and 2018 *IEEE IGARSS Symposium Prize Paper Awards* and 2019 *WHISPER Outstanding Paper Award*. He was the Guest Co-Editor of many Special Issues of international journals. He is the Co-Founder of the IEEE International Workshop on the Analysis of Multi-Temporal Remote-Sensing Images (MultiTemp) series and is currently a Member of the Permanent Steering Committee of this series of workshops. Since 2003, he has been the Chair of the SPIE Conference on Image and Signal Processing for Remote Sensing. He has been the founder of the IEEE GEOSCIENCE AND REMOTE SENSING MAGAZINE for which he was the Editor-in-Chief between 2013 and 2017. He is currently an Associate Editor for the IEEE TRANSACTIONS ON GEOSCIENCE AND REMOTE SENSING. Between 2012 and 2016, he was a Distinguished Speaker of the IEEE Geoscience and Remote Sensing Society.